CORRIGENDUM

M. C. GREGG AND G. S. CARTER

Applied Physics Laboratory and School of Oceanography, University of Washington, Seattle, Washington

E. KUNZE

School of Earth and Ocean Sciences, University of Victoria, Victoria, British Columbia, Canada

(Manuscript received in final form 12 April 2005)

ABSTRACT

Corrected numbers and figures for mixing rates are given for two papers by the authors about Monterey submarine canyon.

1. The error

Many dissipation rates ε and corresponding diapycnal diffusivities K_ρ in Carter and Gregg (2002) and Kunze et al. (2002) were overestimated. The problem occurred with data from the deep Advanced Microstructure Profilers (AMPs) because the electronics gain used during processing was a factor of 2 smaller than the instrument's gain. Because ε estimates are inversely proportional to the square of the gain used during processing, the estimates were at least 4 times too large. Larger dissipations ($\varepsilon \geq 10^{-6}$ W kg^{-1}) required a larger correction (up to a factor of 10) because the upper-wavenumber cutoff of the variance integration depends on signal level for the larger signals (Wesson and Gregg 1994). The combination of a high mixing environment and the lognormal nature of ε results in averages being reduced about a factor of 6. The error affects all of the microstructure data in Kunze et al. (2002) and two-thirds of the data in Carter and Gregg (2002) because this work also used data from our Modular Microstructure Profiler (MMP) instruments, which were not affected by the mistake.

2. Corrections to Carter and Gregg (2002)

The cruise-average dissipation rate in the canyon becomes $\bar{\varepsilon} = 1.9 \times 10^{-7}$ W kg^{-1} (from 1.1×10^{-6}), and

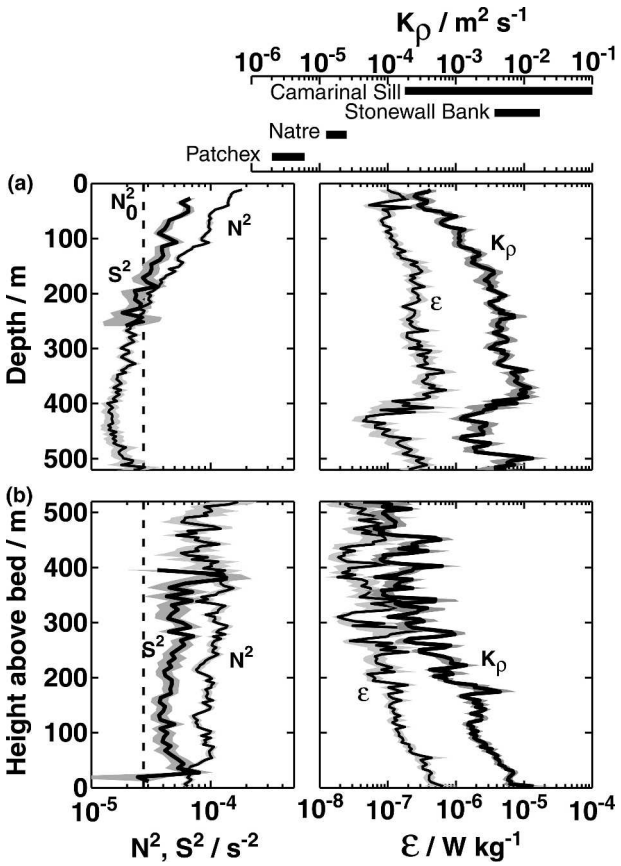

FIG. 1. Averages of profiles taken within 15 km of Moss Landing [replacing Fig. 1 in Carter and Gregg (2002)] plotted (a) vs depth and (b) vs height above bed. The K_ρ axis includes ranges from other sites reported in the literature. Gray shading gives 95% bootstrap confidence limits, and $N_0 = 0.0052$ s^{-1}.

Corresponding author address: M. C. Gregg, Applied Physics Laboratory, University of Washington, 1013 NE 40th St., Seattle, WA 98105.
E-mail: gregg@apl.washington.edu

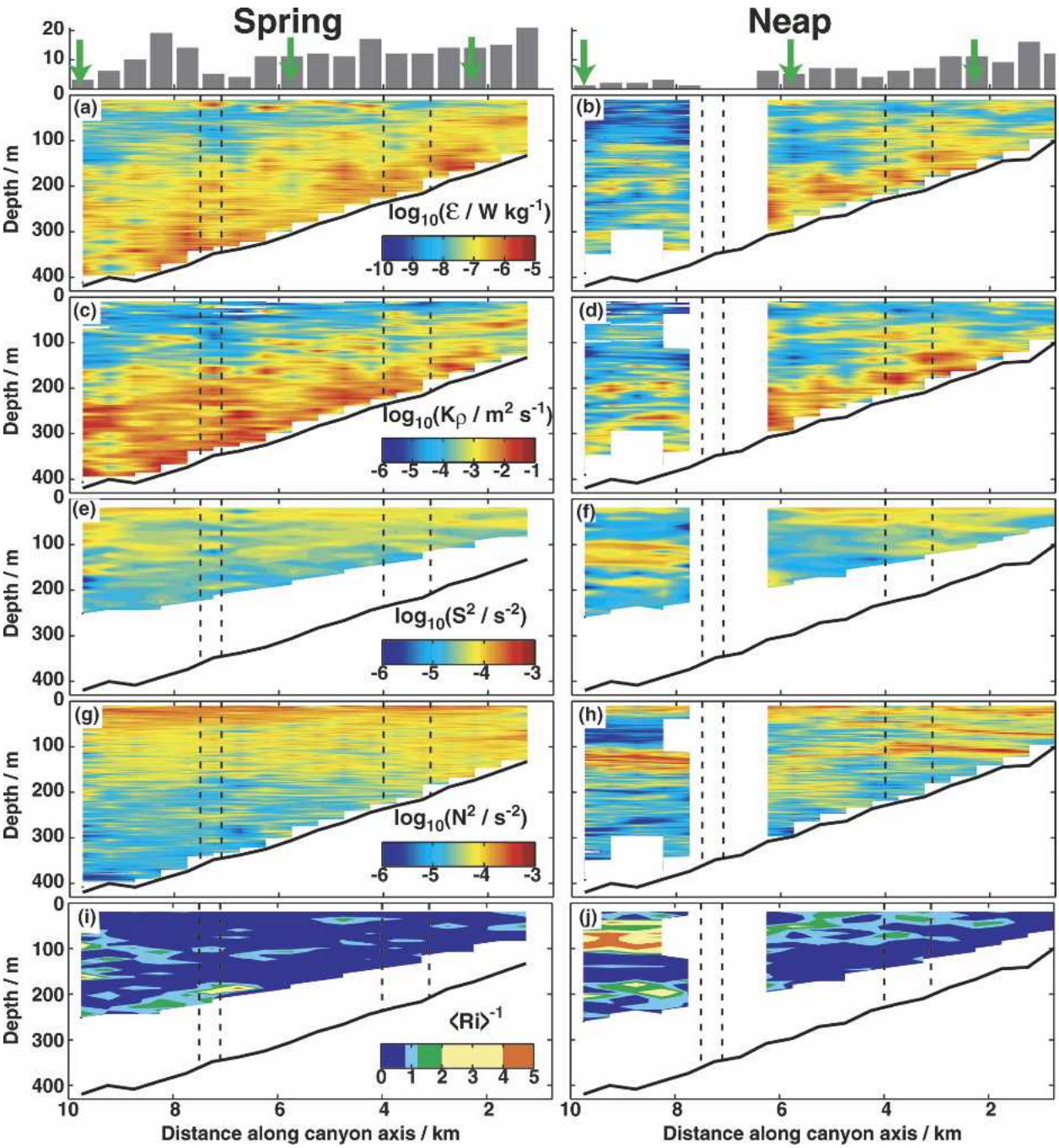

FIG. 2. Along-canyon bin averages of ε, K_ρ, S^2, N^2, and Ri^{-1} during (left) spring and (right) neap tides [replacing Fig. 6 in Carter and Gregg (2002)]. Histograms show the number of profiles in the 500-m averages; only drops within 250 m of the canyon axis were included. Green arrows show the location of sample profiles plotted in their Figs. 7 and 8, and the dashed vertical lines mark the location of major meanders in the canyon axis.

the corresponding diapycnal diffusivity becomes $\overline{K_\rho} = 2.5 \times 10^{-3}$ m^2 s^{-1} (from 1.0×10^{-2}). The crude extrapolation to global dissipation in canyons decreases to 12 GW (from 58 GW), corresponding to ≈3% of global dissipation by the M_2 internal tide (from 15%).

Replacing Fig. 5 in the original paper, Fig. 1 compares cruise-average profiles with ranges from other locations often cited in the literature. Shapes of the profiles are unchanged, but their magnitude decreased relative to mixing at the reference locations. Even so,

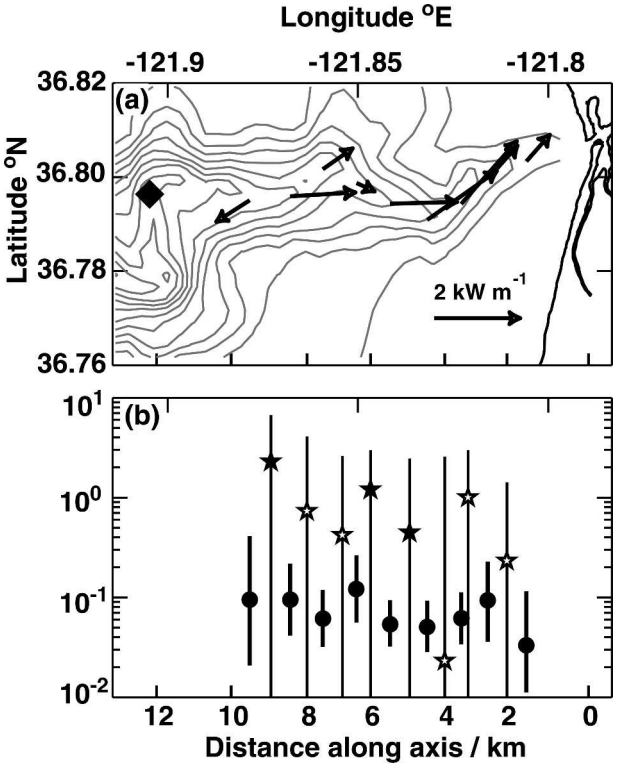

FIG. 3. (a) Vertically integrated energy fluxes during spring tide in 1-km along-canyon bins [repeating Fig. 12a in Carter and Gregg (2002)]. The diamond marks the only place where Kunze et al. (2002) found a seaward flux in the canyon. (b) Comparison of vertically integrated energy flux convergences (open stars) and divergences (closed stars) with vertically integrated turbulent production rates [solid circles; replacing Fig. 12b in Carter and Gregg (2002)]. Vertical lines are error estimates of one standard deviation. The corrected turbulent production rates are now at least a decade lower than the convergences and divergences of the energy flux.

the canyon averages are close to the largest averages reported.

Reduction of the contrast between spring and neap average sections is the only significant change in pattern resulting from correction. This occurred because all the spring data were taken with deep AMPs, but most of the neap data were taken with MMPs, which were not affected by the error. During spring tide $\overline{\varepsilon} = 2.6 \times 10^{-7}$ W kg^{-1} [(2.5–2.7) $\times 10^{-7}$ 95% confidence limits] (from 1.8×10^{-6}), and $\overline{K_\rho} = 3.8 \times 10^{-3}$ m^2 s^{-1} [(3.6–3.9) $\times 10^{-3}$] (from 1.3×10^{-2}). During neap tide $\overline{\varepsilon} = 1.8 \times 10^{-7}$ W kg^{-1} [(1.7–2.0) $\times 10^{-7}$] (from 2.5×10^{-7}), and $\overline{K_\rho} = 2.3 \times 10^{-3}$ m^2 s^{-1} [(2.1–2.5) $\times 10^{-3}$] (from 2.6×10^{-3}). The contrast in magnitude is not quite 50%, much less than the sevenfold difference in the original estimate. However, contours along the canyon axis of spring/neap average profiles show that the region of strong mixing during spring tide remains thicker than the one during neap, extending more than 200 m above the bed as compared with about 100 m (Fig. 2).

Vertically integrated dissipation rates are now 1/3–1/20 of the magnitude of the divergences and convergences of the up-canyon energy flux (Fig. 3), though within the error bars. The discrepancy may be due to undersampling; the inability of the acoustic Doppler current profiler (ADCP) to measure near the bed, making the energy-flux estimates unreliable; energy-flux convergences and divergences raising and lowering the internal wave energy level—that is, $\partial E/\partial t$; or energy fluxes crossing the canyon walls.

When plotted against shear (Fig. 4), the corrected

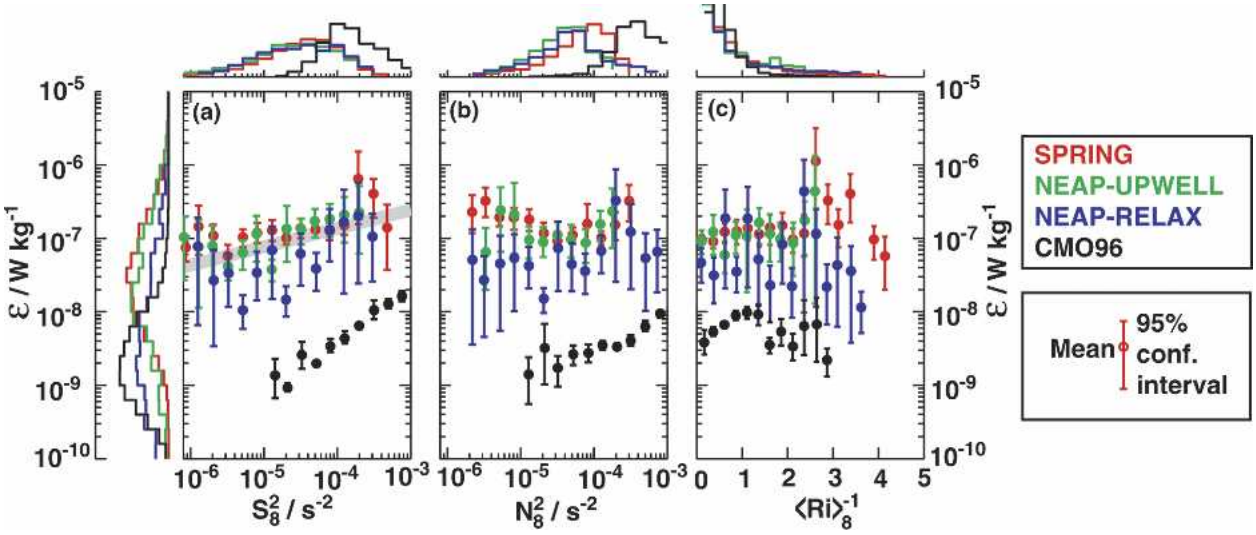

FIG. 4. Dissipation averaged into logarithmically even bins of (a) S^2, (b) N^2, and (c) Ri^{-1} [replacing Fig. 14 in Carter and Gregg (2002)]. The thick gray line in (a) shows $\varepsilon \propto |S_8|^{0.5}$. Spring and neap data are now much closer together and remain much above observations from the 1996 Coastal Mixing Cruise on the New England shelf (MacKinnon and Gregg 2003).

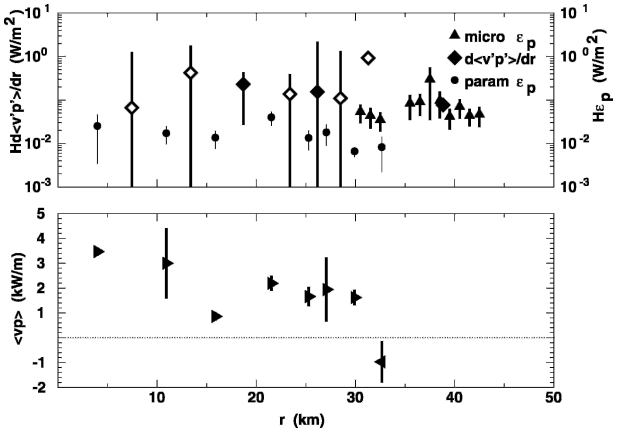

FIG. 5. (top) A test of the hypothesis that turbulence production, $\varepsilon_p = \varepsilon(1 + \gamma)$, along the canyon axis arises from along-canyon convergence of up-canyon energy fluxes $\nabla_{||}\langle \nu'_{||} p' \rangle_\phi$ [replacing Fig. 12 of Kunze et al. (2002)]. Values integrated over the full water column are compared. Open diamonds corresponded to vertically integrated energy flux convergences, $\int_{-H}^{0} (\partial \langle \nu'_{||} p' \rangle_\phi / \partial r_{||})\, dz$, (i.e., an internal wave sink), solid diamonds to divergences (an internal wave source) the solid diamond as 38 km was estimated assuming zero flux at the canyon head. Triangles denote vertically integrated turbulence production rates, $\int_{-H}^{0} \varepsilon_p\, dz$, (assuming a mixing efficiency of $\gamma = 0.2$) and dots vertically integrated turbulence production rates using the Polzin et al. (1995) parameterization. Vertical bars about the symbols correspond to one standard deviation about the station means. (bottom) Vertically integrated energy fluxes $\int_{-H}^{0} \langle \nu'_{||} p' \rangle_\phi\, dz$ along the canyon axis.

dissipation rates retain their lower sensitivity to shear, $\varepsilon \propto |S_8|^{0.45}$, as compared with $\varepsilon \propto |S_8|^{1.4}$ on the New England shelf (MacKinnon and Gregg 2003) and $\varepsilon \propto |S_{10}|^4$ in the open ocean (Gregg 1989).

A pdf of the revised paper is posted online at http://opd.apl.washington.edu/scistaff/bios/gregg/gregghome.html.

3. Corrections to Kunze et al. (2002)

Deeper along the canyon axis (axis depths 500–1500 m), Kunze et al. (2002) also compared energy-flux convergences and divergences with turbulence production rates $\varepsilon_p = \varepsilon(1 + \gamma)$, where γ is the mixing efficiency. With the corrections, vertically integrated dissipation rates are closer to estimates employing the finescale parameterization of Polzin et al. (1995) but still significantly higher (Fig. 5). The energy-flux divergence (solid diamonds, internal wave source) at 38 km from the shelf break is of comparable magnitude to neighboring dissipation rates. The energy-flux convergence (open diamonds, internal wave sink) at 31 km is over an order-of-magnitude larger than neighboring dissipation estimates. The energy-flux convergence at 28 km is closer in magnitude. In both cases, uncertainties in the energy-flux convergence are large enough so that the flux convergence and dissipation estimates are not significantly different. However, energy-flux convergences appear to exceed the dissipation rates. As already mentioned, such discrepancies could arise because of energy-flux convergences being partly balanced by changes in the internal wave energy level, $\partial E/\partial t$, or by fluxes across the canyon walls. The microstructure measurements may also miss strong dissipation contributions from the bottom few meters.

A pdf of the revised paper will be posted on E. Kunze's Web site being prepared at the University of Victoria.

REFERENCES

Carter, G., and M. Gregg, 2002: Intense, variable mixing near the head of Monterey submarine canyon. *J. Phys. Oceanogr.,* **32,** 3145–3165.

Gregg, M., 1989: Scaling turbulent dissipation in the thermocline. *J. Geophys. Res.,* **94,** 9686–9698.

Kunze, E., L. Rosenfeld, G. Carter, and M. Gregg, 2002: Internal waves in Monterey submarine canyon. *J. Phys. Oceanogr.,* **32,** 1890–1913.

MacKinnon, J., and M. Gregg, 2003: Mixing on the late-summer New England shelf—Solibores, shear, and stratification. *J. Phys. Oceanogr.,* **33,** 1476–1492.

Polzin, K., J. M. Toole, and R. W. Schmitt, 1995: Finescale parameterization of turbulent dissipation. *J. Phys. Oceanogr.,* **25,** 306–328.

Wesson, J., and M. Gregg, 1994: Mixing at Camarinal Sill in the Strait of Gibraltar. *J. Geophys. Res.,* **99,** 9847–9878.